Available online at www.eccomasproceedia.org
Eccomas Proceedia SMART (2023) 1722-1731

ECCOMAS
Proceedia

X ECCOMAS Thematic Conference on Smart Structures and Materials
SMART 2023
D.A. Saravanos, A. Benjeddou, N. Chrysochoidis and T. Theodosiou (Eds)

A SOFT FREE SHAPE CASTED PIEZOELECTRIC ELASTOMER

LORENZO NICOLINI*, ANDREA SORRENTINO* AND DAVIDE CASTAGNETTI*

* University of Modena and Reggio Emilia
Department of Engineering Sciences and Methods, Machine Design Group (MDG)
Via G. Amendola 2 Reggio nell'Emilia, Italy
e-mail: lorenzo.nicolini@unimore.it, www.machinedesign.re.unimore.it

Abstract. Piezoelectric materials are largely used for sensing and energy harvesting applications as simple and reliable solutions from piezoelectric accelerometers to vibration energy harvesters. Most of the applications utilize either piezoceramic materials, exploiting their high piezoelectric coefficients, or piezoelectric polymers, thanks to their soft response, in applications where finite displacements are needed.
Actual piezoceramic materials are expensive, brittle and available only in standard and flat shapes. On the other hand, piezoelectric polymers, like PVDF, are too stiff for many applications that need softer solutions.
This work presents the study, development and validation of a new soft piezoelectric elastomer, which can be designed in free shape through a casting process. This study identified a novel formulation of a cold polymerizable silicone-based elastomer, enhanced with BaTiO3 (barium titanate) powder.
A detailed procedure of fabrication was defined involving the mixture preparation, curing and polarization phases of the solution. To obtain disk specimen, we designed and used a dedicated 3D printed acrylonitrile butadiene styren (ABS) mold with a cylindrical cavity. The mold houses two steel electrodes for the polarization through a high voltage DC converter. This allows to perform the polarization process at the same time of the polymerization in order to easily orientate polar BaTiO3 particles in the liquid solution until the polymerization is completed.
To experimentally evaluate the effect of the main variables on the fabrication procedure and the piezopolymer response, we conducted a systematic test plan. Specifically, we investigated both the effect of barium titanate powder concentration and voltage polarization level on the morphological appearance of the specimen and on its piezoelectric properties. Two quasistatic cyclic compression tests at different strain levels were performed on small cylindrical samples cut by the specimens, registering the mechanical behaviours and electric voltage output signals. The piezoelectric coefficient d_{33}, calculated for all the configurations and for both strain levels, highlights a remarkable performance of the proposed piezoelectric polymer.

Key words: Piezoelectric, Elastomer, Sensing, Energy Harvesting, Polarization, Polymerization.

Peer-review under responsibility of the organizing committee of SMART 2023.
doi: 10.7712/150123.9943.450540

1 INTRODUCTION

Common piezoelectric materials are largely used for countless applications, in the form of sensors [1]–[4], actuators [5], [6], energy harvesters [7]–[9] etc. Among the most common piezoelectric materials we find piezoceramics which claim very high piezoelectric performances but they are generally expensive, extremely rigid and brittle, and thus, not suitable in applications where high strains are involved. On the other hand, commercial MFCs are flexible piezoelectric films which take place where rigid piezoelectric elements fail [10]–[13]. Piezopolymers also play an important role in the field of elastic high strain piezoelectric, despite of the lower performances. Despite of that, all the commercial piezoelectric are all available in flat and thin surfaces with limited geometries.

Recent researches aim to find new flexible and soft piezoelectric structures with different geometries. Many researchers have found ad-hoc flexible or soft solutions specifically for health condition monitoring, sport wear, equipment and human motion control. Furthermore, other have investigated possibilities to obtain free thin shapes, generally 3D surfaces, of flexible piezoelectric elements [14]–[22]. Others have designed new interesting methods and procedures to fabricate bulky and soft piezoelectric elements for a wide range of applications but with complex and elaborated fabrication methods with further temperature treatments[23], [24].

In order to overcome these issues and moving towards a simpler fabricability, we developed a new free shape easy castable piezo-elastomer with a bulky structure for a large range of applications. This study reports the design, development and a detailed procedure of fabrication of a new soft piezopolymer based on a silicone polymerizable matrix enhanced with a 99% pure barium titanate powder ($BaTiO_3$) [25] This solution exploits the simultaneous process of curing and poling: polar particles are easily orientable when the mixture is liquid. Once the solution polymerized, the oriented particles are stuck into the rubber and no longer movable.

The Sylgard 184 liquid silicone [26] is mixed with its chemical reagent in a solution with an addition of a prescribed quantity of piezoceramic charge. The liquid solution in casted in a dedicated 3D printed mold which houses two metallic electrodes as inserts, connected to an external high voltage power supply. After an air evacuation phase, the solution is contemporaneously cured and poled at ambient temperature for approximately 30 hours.

Our mold is characterized by an internal cylindric cavity to obtain small piezo-elastic compression test specimens with an external diameter of 16.4 mm and a height of 2.5 mm.

We conducted a test plan producing different configuration of specimens varying two variables: polarization electric field and weight powder concentration. Morphological appearances have been discussed particularly involving the anisotropy of the powder distribution. Additionally, we mechanically validated all the specimens in cyclic compression tests at two levels of strain. The compression force was directed along the polarization axis and simultaneously we acquired the output voltage signals, obtaining the correspondent piezoelectric coefficients d_{33}. Significant results have been achieved in term of piezoelectric performances considering the extremely softness and hyperelasticity of the components. The possibility to obtain free and 3D bulky shapes makes this material particularly suitable for condition monitoring applications, health monitoring and sensing, sport equipment, soft robotic

and many sensor applications.

2 METHOD

2.1 Materials

The solution recipe comprehends two ingredients. First, the polymeric matrix consists in a bi component polymerizable silicone base sold by Dow Chemical, named Sylgard 184 [26]. This product is composed by a liquid transparent primary component and its chemical reagent with a suggested mixing ratio equal to 10:1. This elastomeric silicone claims a very low hardness (43 Shore A) and a remarkable ultimate tensile strength (6.7 MPa). Second, the piezoelectric agent is a BaTiO3 (barium titanate), 99% pure ceramic powder, with high piezoelectric properties, a formula weight of 233.19 g/mol and density of 6 g/cm^3, and a nominal particle size lower than 3 μm [25].

The choice of this piezoelectric charge comes from its commercially availability and cost among other piezoceramic powders. All silicone products have a density that is around 1 - 1.2 g/cm^3. The Sylgard 184 has been chosen because its considerable viscosity (3.5 $Pa \cdot s$) which avoids powder to settle down on the bottom even with a significant density difference with respect to the piezoelectric charge.

2.2 Procedure

The fabrication procedure consists in three sequential and easy steps: mixture preparation, air evacuation phase and polarization and curing phase. The procedure does not depend on the chosen shape and can be applied for different molds with some cautions on the air evacuation phase.

First, the piezoelectric powder is mixed to the silicone matrix through a mixer, inside a bowl, for a time of 3 minutes. Once the powder completely diffuses into the liquid silicone, the catalyst has to be added to start the polymerization. After a second mixing lasting 1 minute, the solution is casted into the mold. Second, since mixing processes incorporates air into the liquid, it is necessary to remove bubbles avoiding internal cavities in the final sample. Thus, the whole mold is placed in a vacuum chamber that works with a Venturi valve, receiving the air flow from an air compressor. The vacuum pressure has to be sufficient to remove air bubbles. Dependently on the mold geometry, the pressure and time of degasification may change. In our case, to obtain the best results, the air evacuation process was repeated two times, ten minutes long each with a negative pressure of 0.88 bar. Third, we performed the polarization of the specimen by applying an electric potential to the electrodes. The electric potential came from a series of two power supply: a first power supply (AIM-TTi CPX400A Dual 60V/20A [27]) converts power from the supply network (220V, AC) to an output signal of 12 V DC; this output voltage becomes inputs to a high voltage DC-DC converter (XP Power Emco high voltage

corporation - CB101 [28]), which provides an output voltage up to 10 kV. A potentiometer applied to this second device allowed to continuously regulate the output voltage. Positive and negative output voltage cables from the high-tension converter were welded to the electrodes. Simultaneously, the silicone polymerization occurred in a controlled ambient temperature through a climatic chamber for 30 hours, a curing time that according to the silicon manufacturer ensures a complete curing process. The specimen was then extracted from the mold.

2.3 Mold design

The mold was designed according to our needs. Our internal cavity consists in a cylindric room for the realization of compression test specimens. The mold is composed by four parts: two 3D printed acrylonitrile butadiene styren (ABS) plastic parts (upper and lower part) where to house an upper and lower steel electrode. The two electrodes are welded to the high voltage power supply which provides the electric field for the polarization. ABS plastic parts are important to electrically insulate the two electrodes avoiding undesired parasite current between them. In order to facilitate the air evacuation process, we created three exhaust duct equispaced at 120 degrees on the upper mold plastic part. These three elements connect the lateral surface of the cylindric cavity with the outside. Figure 1 illustrates the mold schematic with principal dimensions.

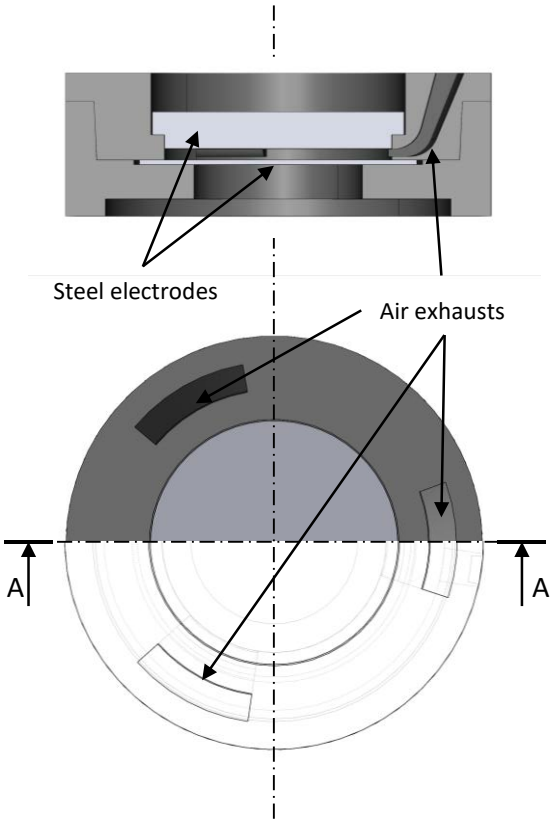

Figure 1: Mold schematic assembly: upper and section view of the assembled mold.

3 CONFIGURATIONS INVESTIGATED

The test plan investigated the effect of two variables related to the procedure of fabrication on three levels: polarization voltage (0, 2 and 4 kV) and piezoelectric charge concentration (25%, 50%, 65% by weight). It comes a matrix of nine configurations. For each of them we repeated the procedure three times selecting the best sample in terms of external surface and number of imperfections. In the most of the castings external small imperfection are present on the lateral surface with the issue to have different surface areas. For this reason, we extracted smaller cylinders from the casted specimen with a die cutting operation, excluding the external edge. We got 9 identical good quality specimens with a diameter of 16.4 mm and a height around 2.5 mm. All the specimen morphological appearances were checked through an optical Image Dimension Measurement System (Keyence IM-8030). Figure 2 shows all the configurations investigated.

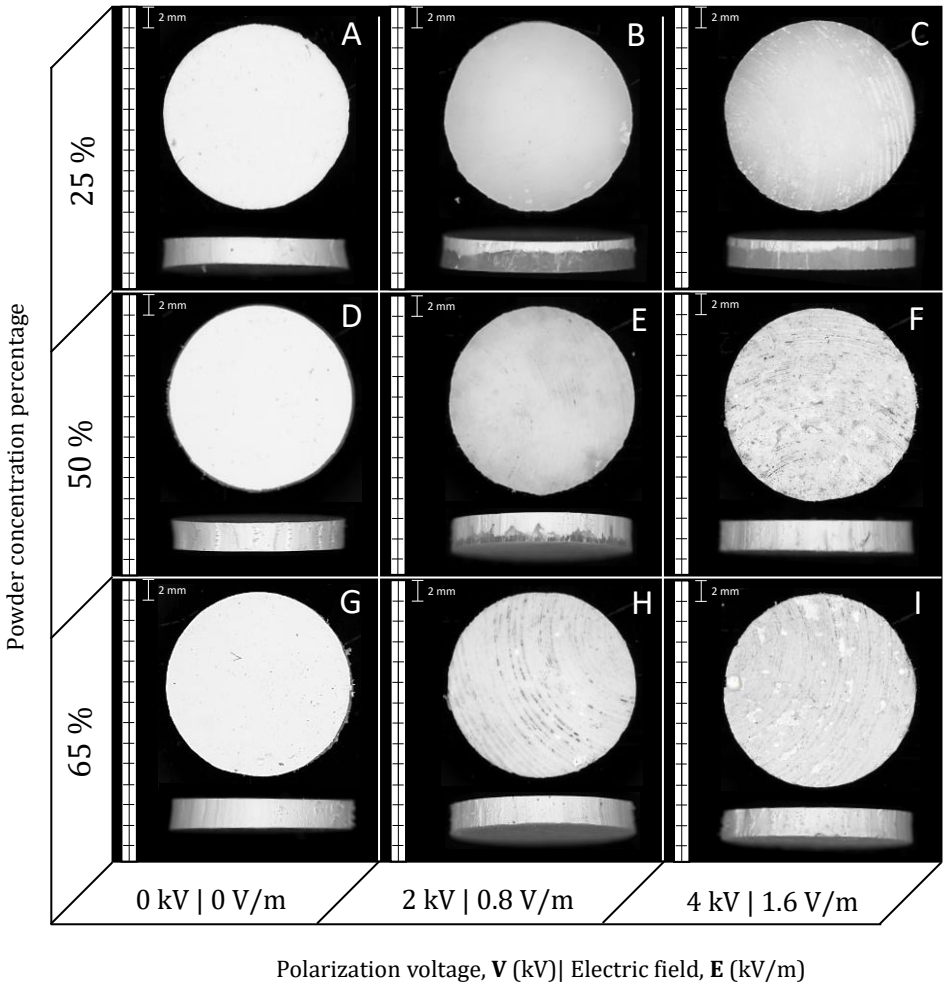

Figure 2: Specimen configurations investigated. Three levels of polarization voltage / electric field: 0, 2, 4 kV (0, 0.8, 1.6 kV/m). Three levels of powder concentration by weight: 25%, 50% and 65%.

Not polarized specimens, shown in the left column in Figure 2 (A, D and G), appear very similar to each other despite of the different powder concentration: BaTiO3 diffused in the silicone base creating opaque white specimens in all the three cases shown. On the other hand, polarized specimens are characterized by two different layers. Since unpolarized specimens presented uniform appearances, the electric field must be the cause of separated separation of the mixture in two parts: on the left side the powder has been attracted keeping more transparent the right side. This effect is visible only in specimens with a low powder concentration.

4 EXPERIMENTAL ASSESSMENT

The experimental assessment aimed to characterize the realized configurations under cyclic compression test acquiring both mechanical and electrical behaviours in order to obtain the main piezoelectric coefficient d_{33}.

4.1 Test bench

The test bench is constituted by an electromechanical Galdabini Sun 500 [29] as characterization compression machine that exerts the compression forces through two electrical insulated steel plates. Each specimen was equipped of two conductive aluminum sheets on both circular faces, furtherly wired in parallel to a 70 MΩ. The voltage was acquired by a NI acquisition board ([30]) on the two resistor ends. All the data were collected by a notebook. Figure 3 illustrates the test bench configuration.

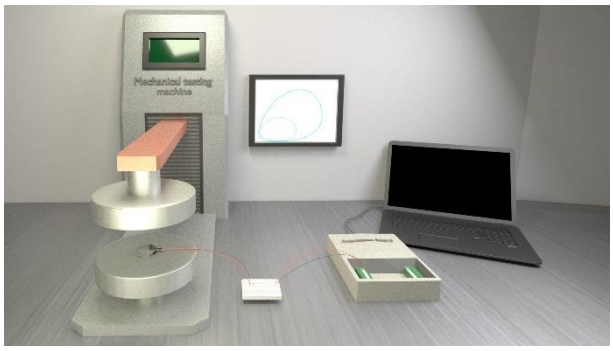

Figure 3: Rendering picture of the test bench set up

4.2 Test procedure

The tests investigated two strain levels, ε_m, equal to 25% and 40% of the specimen thickness. The compression tests involved two consecutive steps. First, a quasi-static linear ramp that compresses the specimen up to half of the total desired strain ($\frac{\varepsilon_m}{2}$), with a speed of 1 mm/min. Second, starting from the previous deformation, a cyclic compression with a sine displacement

law having an amplitude equal to $\frac{\varepsilon_m}{2}$ and a frequency of 0.5 Hz. This last step applies a cyclic compression on the specimen from zero up to ε_m of its thickness.

The d_{33} coefficient was obtained by

$$d_{33} = \frac{Q}{F} \tag{1}$$

where Q is the electric charge provided by the piezo-elastomer specimen and F is the maximum vertical compression force exerted by the machine.

5 RESULTS

The most interesting result consists in the d_{33} piezoelectric coefficient. Figure 4 compares the inducted polarization obtained in the investigated configurations.

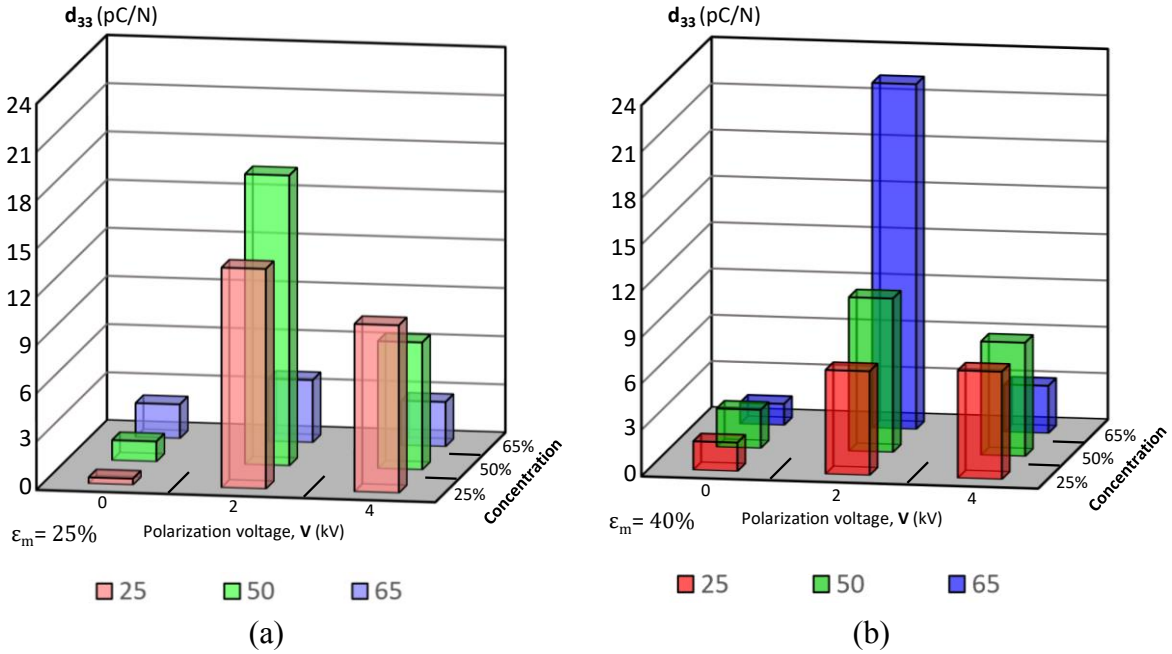

Figure 4: Induced polarization d_{33} at 25% (a) and 40 % (b) of compression strain in the nine configurations.

The bar charts shows that the presence of the electric field is strongly recommended to increase the piezoelectric performances. However, the achieved results are not linearly related to the electric field intensity. As shown in Figure 4 the d_{33} piezoelectric coefficient does not increase consistently or even decreases when the polarization voltage doubles.

On the other side, the powder concentration also plays a crucial role. Figure 4 clearly shows that high amounts of powder concentration reduce the piezoelectric coefficient mainly because the correspondent specimens are more rigid and harder and they require an higher compression force to reach the same strain level.

Despite of the low voltage polarization applied, this piezopolymer shows a d_{33} piezoelectric coefficient higher than other not brittle materials, like unpoled and poled β-phase PVDF and comparable with poled β-phase PVDF-TrFE.

CONCLUSIONS

This work reports the study, development and validation of a soft piezo-polymer with enhanced piezo-elastic response and easy castable in a free shape. Specifically, the work identified a new formulation for soft piezopolymers based on ambient temperature polymerizable silicone rubber mixed with BaTiO3 ceramic powder, castable in 3D printed plastic molds.

Through a full factorial test plan, we experimentally investigated the effect of powder concentration and voltage polarization over three levels. For each of the nine configurations investigated, a thin cylindrical specimen was casted, cured and polarized in an ad-hoc designed mold. To evaluate their mechanical and piezoelectric response, we performed cyclic compression tests at two maximum strain levels, registering both their force-displacement characteristic and the output voltage through a specific electrical circuit. The results allowed to identify the optimum configurations in terms of piezoelectric coefficient d_{33}.

It worth noting that piezoelectric performances are higher than other not brittle materials and comparable with β-phase structure PVDF. In addition, this piezopolymer stands out for its extremely stretchable response and its low hardness ensuring large strains without any damage. These characteristics make this piezopolymer particularly suitable for sensors or transductors in multiple application fields, such as health conditions monitoring, mechanical applications, sport wear and equipment, soft robotics and human motion sensing applications.

REFERENCES

[1] S. Tadigadapa and K. Mateti, "Piezoelectric MEMS sensors: state-of-the-art and perspectives," *Meas Sci Technol*, vol. 20, no. 9, p. 092001, 2009, doi: 10.1088/0957-0233/20/9/092001.

[2] G. Gautschi, "Piezoelectric Sensors," in *Piezoelectric Sensorics: Force Strain Pressure Acceleration and Acoustic Emission Sensors Materials and Amplifiers*, G. Gautschi, Ed., Berlin, Heidelberg: Springer Berlin Heidelberg, 2002, pp. 73–91. doi: 10.1007/978-3-662-04732-3_5.

[3] M. Varanis, A. Silva, A. Mereles, and R. Pederiva, "MEMS accelerometers for mechanical vibrations analysis: a comprehensive review with applications," *Journal of the Brazilian Society of Mechanical Sciences and Engineering*, vol. 40, no. 11, p. 527, 2018, doi: 10.1007/s40430-018-1445-5.

[4] E. J. Curry *et al.*, "Biodegradable Piezoelectric Force Sensor," *Proceedings of the National Academy of Sciences*, vol. 115, no. 5, pp. 909–914, Jan. 2018, doi: 10.1073/pnas.1710874115.

[5] S. Mohith, A. R. Upadhya, K. P. Navin, S. M. Kulkarni, and M. Rao, “Recent trends in piezoelectric actuators for precision motion and their applications: a review,” *Smart Mater Struct*, vol. 30, no. 1, p. 013002, Jan. 2021, doi: 10.1088/1361-665X/abc6b9.

[6] X. Gao *et al.*, “Piezoelectric Actuators and Motors: Materials, Designs, and Applications,” *Adv Mater Technol*, vol. 5, no. 1, p. 1900716, Jan. 2020, doi: 10.1002/admt.201900716.

[7] D. Castagnetti, “Experimental modal analysis of fractal-inspired multi-frequency structures for piezoelectric energy converters,” *Smart Mater Struct*, vol. 21, no. 9, p. 094009, Sep. 2012, doi: 10.1088/0964-1726/21/9/094009.

[8] D. Castagnetti, “Fractal-Inspired Multifrequency Structures for Piezoelectric Harvesting of Ambient Kinetic Energy,” *Journal of Mechanical Design*, vol. 133, no. 11, Nov. 2011, doi: 10.1115/1.4004984.

[9] D. Castagnetti and E. Radi, “A piezoelectric based energy harvester with dynamic magnification: modelling, design and experimental assessment,” *Meccanica*, vol. 53, no. 11–12, pp. 2725–2742, Sep. 2018, doi: 10.1007/s11012-018-0860-0.

[10] Z. Zheng *et al.*, “Model-Based Control of Planar Piezoelectric Inchworm Soft Robot for Crawling in Constrained Environments,” in *2022 IEEE 5th International Conference on Soft Robotics (RoboSoft)*, IEEE, Apr. 2022, pp. 693–698. doi: 10.1109/RoboSoft54090.2022.9762147.

[11] A. S. Barbosa, L. Z. Tahara, and M. M. da Silva, “Motion planning of a fish-like piezoelectric actuated robot using model-based predictive control,” *Journal of Vibration and Control*, vol. 29, no. 1–2, pp. 411–427, Jan. 2023, doi: 10.1177/10775463211048255.

[12] H. B. Lee, Y. W. Kim, J. Yoon, N. K. Lee, and S.-H. Park, “3D customized and flexible tactile sensor using a piezoelectric nanofiber mat and sandwich-molded elastomer sheets,” *Smart Mater Struct*, vol. 26, no. 4, p. 045032, Apr. 2017, doi: 10.1088/1361-665X/aa64ca.

[13] M. Pan *et al.*, “Piezoelectric-Driven Self-Sensing Leaf-Mimic Actuator Enabled by Integration of a Self-Healing Dielectric Elastomer and a Piezoelectric Composite,” *Advanced Intelligent Systems*, vol. 3, no. 8, p. 2000248, Aug. 2021, doi: 10.1002/aisy.202000248.

[14] S. Hu, Z. Shi, W. Zhao, L. Wang, and G. Yang, “Multifunctional piezoelectric elastomer composites for smart biomedical or wearable electronics,” *Compos B Eng*, vol. 160, pp. 595–604, Mar. 2019, doi: 10.1016/j.compositesb.2018.12.077.

[15] J. Seo *et al.*, “All-organic piezoelectric elastomer formed through the optimal cross-linking of semi-crystalline polyrotaxanes,” *Chemical Engineering Journal*, vol. 426, p. 130792, Dec. 2021, doi: 10.1016/j.cej.2021.130792.

[16] X. Cheng, Y. Gong, Y. Liu, Z. Wu, and X. Hu, “Flexible tactile sensors for dynamic triaxial force measurement based on piezoelectric elastomer,” *Smart Mater Struct*, vol. 29, no. 7, p. 075007, Jul. 2020, doi: 10.1088/1361-665X/ab8748.

[17] D. Khastgir and K. Adachi, “Piezoelectric and dielectric properties of siloxane elastomers filled with bariumtitanate,” *J Polym Sci B Polym Phys*, vol. 37, no. 21, pp. 3065–3070, Nov. 1999, doi: 10.1002/(SICI)1099-0488(19991101)37:21<3065::AID-

POLB15>3.0.CO;2-2.
[18] X. Wang *et al.*, "Highly stretchable lactate-based piezoelectric elastomer with high current density and fast self-healing behaviors," *Nano Energy*, vol. 97, p. 107176, Jun. 2022, doi: 10.1016/j.nanoen.2022.107176.
[19] X. Chou *et al.*, "All-in-one filler-elastomer-based high-performance stretchable piezoelectric nanogenerator for kinetic energy harvesting and self-powered motion monitoring," *Nano Energy*, vol. 53, pp. 550–558, Nov. 2018, doi: 10.1016/j.nanoen.2018.09.006.
[20] X. Wang *et al.*, "A highly efficient piezoelectric elastomer with a green product cycle from fabrication to degradation," *J Mater Sci*, vol. 58, no. 11, pp. 4840–4852, Mar. 2023, doi: 10.1007/s10853-023-08349-y.
[21] A. Cafarelli *et al.*, "Small-caliber vascular grafts based on a piezoelectric nanocomposite elastomer: Mechanical properties and biocompatibility," *J Mech Behav Biomed Mater*, vol. 97, pp. 138–148, Sep. 2019, doi: 10.1016/j.jmbbm.2019.05.017.
[22] Y. Liu *et al.*, "Electronic Skin from High-Throughput Fabrication of Intrinsically Stretchable Lead Zirconate Titanate Elastomer," *Research*, vol. 2020, Jan. 2020, doi: 10.34133/2020/1085417.
[23] S. Mamada, N. Yaguchi, M. Hansaka, M. Yamato, and H. Yoshida, "Performance improvement of piezoelectric-rubber by particle formation of linear aggregates," *J Appl Polym Sci*, vol. 131, no. 3, Feb. 2014, doi: https://doi.org/10.1002/app.39862.
[24] R. Fu *et al.*, "Intrinsically piezoelectric elastomer based on crosslinked polyacrylonitrile for soft electronics," *Nano Energy*, vol. 103, p. 107784, Dec. 2022, doi: 10.1016/j.nanoen.2022.107784.
[25] https://pubchem.ncbi.nlm.nih.gov/substance/24852494. 2023/04/10
[26] https://www.dow.com/documents/en-us/productdatasheet/11/11-31/11-3184-sylgard-184-elastomer.pdf. 2023/04/10
[27] https://www.aimtti.com/. 2023/04/10
[28] https://www.xppower.com/. 2023/04/10
[29] https://www.galdabini.it/. 2023/04/10
[30] https://www.ni.com/en-ca/support/model.usb-6251.html. 2023/04/10